Cancer Cell
Article

A Lymphotoxin-Driven Pathway to Hepatocellular Carcinoma

Johannes Haybaeck,[1,16] Nicolas Zeller,[1,15,16] Monika Julia Wolf,[1] Achim Weber,[2] Ulrich Wagner,[3] Michael Odo Kurrer,[4] Juliane Bremer,[1] Giandomenica Iezzi,[5] Rolf Graf,[6] Pierre-Alain Clavien,[6] Robert Thimme,[7] Hubert Blum,[7] Sergei A. Nedospasov,[8,9] Kurt Zatloukal,[10] Muhammad Ramzan,[11] Sandra Ciesek,[12] Thomas Pietschmann,[12] Patrice N. Marche,[11] Michael Karin,[13] Manfred Kopf,[5] Jeffrey L. Browning,[14] Adriano Aguzzi,[1] and Mathias Heikenwalder[1,*]

[1]Department of Pathology
[2]Institutes of Neuropathology and Clinical Pathology
University Hospital Zurich, CH 8091 Zurich, Switzerland
[3]Functional Genomics Center Zurich, University Zurich, CH 8057 Zurich, Switzerland
[4]Department of Pathology, Cantonal Hospital Aarau, CH 5001 Aarau, Switzerland
[5]Institute of Integrative Biology, Molecular Biomedicine, Swiss Federal Institute of Technology (ETH), Zurich, Schlieren, CH 8952 Schlieren, Switzerland
[6]Swiss HPB (Hepato-Pancreatico-Biliary) Center, Department of Surgery, University Hospital Zurich, CH 8091 Zurich, Switzerland
[7]Department of Internal Medicine, University of Freiburg, D-79106 Freiburg, Germany
[8]Engelhardt Institute of Molecular Biology, Moscow, 119991, Russia
[9]German Rheumatism Research Center, Berlin, 10117, Germany
[10]Institute of Pathology, Medical University of Graz, A 8036 Graz, Austria
[11]INSERM and Université Joseph Fourier-Grenoble, Unité 823, Institut Albert Bonniot UJF Site Santé BP 170 La Tronche, F 38042 Grenoble, France
[12]Division of Experimental Virology, TWINCORE, Centre for Experimental and Clinical Infection Research, Medical School Hannover (MHH) and the Helmholtz Centre for Infection Research (HZI), D-30625 Hannover, Germany
[13]University of California, San Diego and University of California, Los Angeles, CA 92093-0723, USA
[14]Department of Immunobiology, Biogen Idec, Cambridge, MA 02142, USA
[15]Present address: Department of Neuropathology, University of Freiburg, D-79106 Freiburg, Germany
[16]These authors contributed equally to this work
*Correspondence: mathias.heikenwaelder@usz.ch
DOI 10.1016/j.ccr.2009.08.021

SUMMARY

Hepatitis B and C viruses (HBV and HCV) cause chronic hepatitis and hepatocellular carcinoma (HCC) by poorly understood mechanisms. We show that cytokines lymphotoxin (LT) α and β and their receptor (LTβR) are upregulated in HBV- or HCV-induced hepatitis and HCC. Liver-specific LTαβ expression in mice induces liver inflammation and HCC, causally linking hepatic LT overexpression to hepatitis and HCC. Development of HCC, composed in part of $A6^+$ oval cells, depends on lymphocytes and IKappa B kinase β expressed by hepatocytes but is independent of TNFR1. In vivo LTβR stimulation implicates hepatocytes as the major LT-responsive liver cells, and LTβR inhibition in LTαβ-transgenic mice with hepatitis suppresses HCC formation. Thus, sustained LT signaling represents a pathway involved in hepatitis-induced HCC.

INTRODUCTION

A causal relationship between chronic hepatitis, hepatocellular damage, fibrosis, and carcinogenesis is well established (El-Serag and Rudolph, 2007). Various etiologies, including chronic alcohol consumption, chronic drug abuse, autoimmune disorders, toxins (e.g., aflatoxin B), or infections with hepatotropic viruses (e.g., HBV, HCV), can lead to chronic hepatitis,

SIGNIFICANCE

Pharmacological inhibition of LTβR signaling reduces pathogen- and concavalin A-induced liver injury, whereas LTβR signaling on hepatocytes appears to be beneficial during liver regeneration. We demonstrate that sustained hepatic LT expression in mice can be injurious, causing chronic hepatitis and HCC. Enhanced hepatic LTβR signaling might be of potential clinical relevance because LTβR and its ligands are drastically increased in human HBV- and HCV-induced hepatitis and HCC, compared with normal livers or nonviral, benign liver diseases. Thus, hepatic LT signaling might be advantageous if transiently active during liver regeneration, but detrimental if chronically triggered. We propose that suppression of hepatic LTβR signaling might be beneficial in liver diseases with chronic LTα, LTβ, or LIGHT overexpression.

liver fibrosis, and cirrhosis. HBV and HCV infections are by far the most common cause of chronic hepatitis in humans (Malhi et al., 2006). Chronic HBV and HCV infections are frequently associated with HCC, the most prevalent primary human liver cancer (El-Serag and Rudolph, 2007), and except for HBV infections, liver cirrhosis precedes HCC in most cases. The exact mechanisms driving hepatitis-induced liver cancer remain elusive. Among others, aberrant expression of cytotoxic cytokines is thought to be critically involved (Greten and Karin, 2004; Lee et al., 2005; Lowes et al., 2003; Vainer et al., 2008).

The proinflammatory and homeostatic cytokines LTα and LTβ are members of the tumor necrosis factor (TNF) superfamily. Under physiological conditions, LTs are expressed by activated T-, B-, NK-, and lymphoid tissue inducer cells (Fu et al., 1998; Ware, 2005) and are crucial for organogenesis and maintenance of lymphoid tissues (Rennert et al., 1996; Tumanov et al., 2003). Although LTβ contains a transmembrane domain, LTα is soluble. Consequently, LT can exist as membrane-bound heterotrimers ($LT\alpha_1\beta_2$ or $LT\alpha_2\beta_1$) interacting with LTβR or as soluble secreted homotrimers ($LT\alpha_3$) triggering TNF receptor (TNFR) 1 and TNFR2 and the herpesvirus entry mediator receptor (HVEM) (Browning et al., 1997; Ware, 2005). LTβR and TNFR1 signaling can be activated by the HCV-core protein (Chen et al., 1997; Zhu et al., 1998) involving the canonical or noncanonical NF-κB signaling pathways (Ware, 2005; You et al., 1999). Furthermore, HBV or HCV infections lead to increased hepatic LT expression in vivo and in vitro (Lee et al., 2005; Lowes et al., 2003), and HCV replication has been demonstrated to depend on components of the LTβR signaling pathway in vitro (Ng et al., 2007).

LTs can directly act on hepatocytes, which physiologically express high levels of LTβR but little LT (Browning and French, 2002). T cell-derived LT and LIGHT (LT-like, exhibits inducible expression, competes with HSV glycoprotein D for HVEM, expressed by T-lymphocytes) signaling to hepatocytes controls lipoprotein homeostasis (Lo et al., 2007). In addition, LT signaling is important for liver regeneration through T cell-derived LT expression (Tumanov et al., 2008) and regulates hepatic stellate cell function and wound healing (Ruddell et al., 2008). Thus, hepatic LTβR signaling controls liver homeostasis in both health and disease.

Promotion of HCC formation by chronic inflammatory stimuli has been recapitulated in various animal models. Ablation of the multidrug resistance gene 2 (*mdr2*) induces cholestatic hepatitis and liver cancer (Pikarsky et al., 2004), and administration of the chemical carcinogen diethylnitrosamine (DEN) causes acute liver injury and HCC (Maeda et al., 2005). Liver-specific expression of the hepatitis B surface antigen (HBsAg) in mice demonstrates that chronic immune-mediated liver cell injury is critical for HCC formation (Nakamoto et al., 1998).

Triggering TNFR1 or LTβR induces the classical and alternative NF-κB signaling pathways, which are linked to inflammation-induced carcinogenesis (Greten and Karin, 2004). However, the precise role of these pathways in HCC pathogenesis is controversial (Vainer et al., 2008). Mice lacking IKappa B kinase β (IKKβ) specifically in hepatocytes ($Ikk\beta^{\Delta hep}$) exhibit a marked increase in DEN-induced HCC formation, suggesting a protective function of IKKβ in HCC development (Maeda et al., 2005). In contrast, NF-κB signaling promotes HCC development in $mdr2^{-/-}$ mice, and anti-TNFα treatment is protective (Pikarsky et al., 2004). Interestingly, mice with a hepatocyte-specific deletion of IKKγ (also called NEMO) develop steatohepatitis and HCC (Luedde et al., 2007). Consequently, the role of NF-κB signaling in hepatocarcinogenesis might depend on the mouse model and the type or degree of liver inflammation and injury (Vainer et al., 2008). Here, we investigated a possible causal relationship between sustained hepatic LTβR-signaling, chronic hepatitis, and HCC development.

RESULTS

Upregulation of LTα, LTβ, and LTβR in HBV- or HCV-Infected Human Livers and in HCC

The specific role of LT signaling in the pathogenesis of virus-induced hepatitis and HCC formation is not completely defined. We analyzed transcriptional levels of *LTα*, *LTβ*, *LIGHT*, *TNFα*, *LTβR*, and *TNFR1* in human HBV- or HCV-induced chronic hepatitis and HCC or in nonviral HCC, compared with healthy liver specimens (Figure 1; Figure S1 available with this article online). *LTα*, *LTβ*, and *LTβR* mRNA expression was increased, on average, $\sim 2^7$- to 2^{10}-fold in HBV- or HCV-induced hepatitis and HCC ($p < 0.001$); *LIGHT* transcripts were less, but still significantly, elevated (on average, $\sim 2^3$- to 2^5-fold; $p < 0.001$). Likewise, *TNFR1* mRNA expression was significantly increased in HBV- or HCV-induced hepatitis and HCC (on average, $\sim 2^7$- to 2^9-fold; $p < 0.0001$). In contrast, *TNFα* was only slightly upregulated in HBV-induced hepatitis ($p = 0.04$) but not in HCV-induced hepatitis ($p = 0.3$) and HCC ($p = 0.4$).

In most cases, HCV genotype, degree of inflammation (Knodell score), fibrosis (Metavir score), and liver enzyme levels (ALT; AST) were assessed (Tables S1–S5). Levels of *LTα*, *LTβ*, and *LTβR* mRNA did not correlate with the degree of liver inflammation ($p = 0.5$), fibrosis ($p = 0.5$), patient age ($p = 0.5$), sex ($p = 0.5$), HCV genotype, or type of virus infection (HBV, HCV, HBV/HCV coinfection in the case of some HCC; $p = 0.5$) (Figure S1; data not shown).

To determine whether upregulation of LT ligands and receptors was specific for HBV- or HCV-induced liver diseases, we examined transcript levels in nonviral liver diseases. These included liver disorders with hepatitis (alcoholic steatohepatitis [ASH], cholestasis [CH], primary biliary cirrhosis/autoimmune cholangitis [PBC], and end-stage liver cirrhosis due to alcoholic liver disease [CIR]) and liver diseases without inflammation (steatosis [ST] and focal nodular hyperplasia [FNH]). Additionally, other liver diseases (OLD), such as hemochromatosis/siderosis, Wilson's disease, focal liver fibrosis, α1-antitrypsin deficiency, and nonviral HCC (NVH), were investigated.

Levels of *LTα*, *LTβ*, and *LTβR* mRNA were significantly lower in all nonviral liver diseases analyzed except NVH, compared with virus-induced chronic hepatitis and HCC (*LTα*, $p < 0.0001$; *LTβ*, $p = 0.05$; *LTβR*, $p < 0.0001$; Figure 1; Figure S1). This was true whether or not nonviral liver diseases were associated with inflammation. *LIGHT* and *TNFR1* mRNA expression in nonviral liver diseases including NVH was similar to HBV- or HCV-induced chronic hepatitis and HCC. In contrast, *TNFα* mRNA expression was significantly higher in nonviral liver diseases with inflammation and NVH, compared with healthy livers ($p < 0.0001$) or HBV- or HCV-induced hepatitis and HCC ($p < 0.0001$).

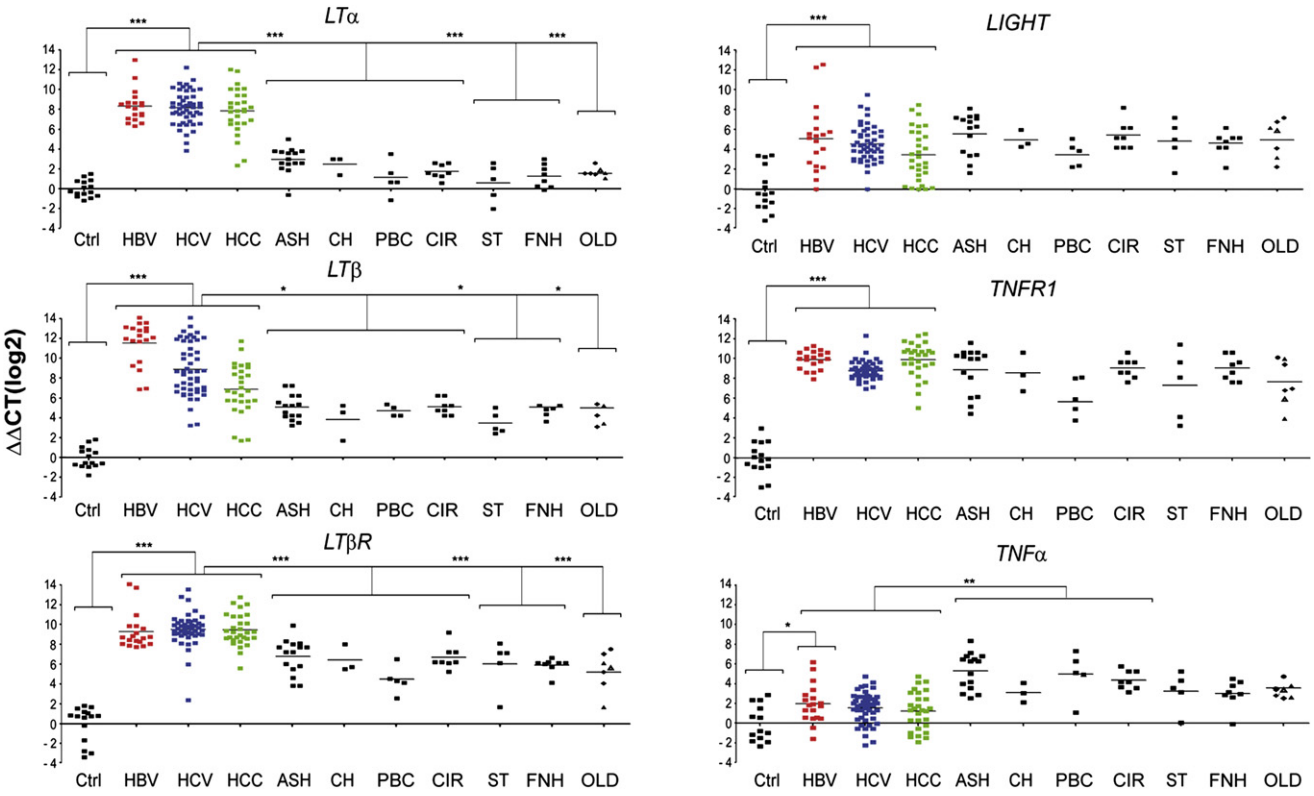

Figure 1. mRNA Expression of Some TNF-Superfamily and TNF-Receptor-Superfamily Members in Viral (HBV- and HCV-Induced) and Nonviral Liver Diseases

Analysis of hepatic *LTα*, *LTβ*, *LTβR*, *LIGHT*, *TNFR1*, and *TNFα* transcription by real-time PCR. Healthy individuals (Ctrl; n = 15), patients chronically infected with HBV (n = 19) or HCV (n = 49), affected by HCC (n = 30), or suffering from various non-virus-related liver disorders were investigated. Non-virus-related liver diseases with hepatitis include alcoholic steatohepatitis (ASH; n = 13), cholestasis (CH; n = 3), primary biliary cirrhosis/autoimmune cholangitis (PBC; n = 5), end-stage liver cirrhosis due to alcoholic liver disease (CIR; n = 8), α1-antitrypsin deficiency (α1AT; n = 1), and focal liver fibrosis (FLF; n = 2). Non-virus-related liver diseases without hepatitis include steatosis (ST; n = 5), hemochromatosis/siderosis (HE/SID; n = 3), and Wilson's disease (WD; n = 1). Focal nodular hyperplasia (FNH; n = 8) was investigated as a benign primary liver tumor. Diseases such as α1AT (black circles), FLF (black triangles), HE/SID (black diamonds), and WD (white diamonds) are listed under "other liver diseases" (OLD). Horizontal bars represent the average mRNA expression level. The *y* axis describes the ΔΔCT values on a $\log_2$ scale. Asterisks indicate statistical significance: *p ≤ 0.05; **p < 0.001; ***p < 0.0001.

Increased Chemokine Expression in HBV- or HCV-Induced Hepatitis and HCC

To confirm that proinflammatory signaling cascades are activated during HBV- or HCV-induced hepatitis and HCC formation, chemokine mRNA levels were measured (Figure S1). *CCL2*, *CCL3*, *CCL5*, and *CXCL10* mRNA expression was significantly higher in human HBV-induced (p < 0.0001) or HCV-induced (p < 0.0001) hepatitis and HCC (p < 0.0001) than in healthy controls. *CXCL1* mRNA expression was significantly increased in HBV-induced hepatitis (p < 0.0001) and HCC (p = 0.02), but not in HCV-induced hepatitis (p = 0.07).

Upregulation of LTα, LTβ, and LIGHT in Human Hepatoyctes upon HCV Infection In Vitro

We next investigated whether *LTα*, *LTβ*, *LIGHT*, and *LTβR* transcripts can be upregulated in hepatocytes as a consequence of viral infection. The human hepatocyte cell line Huh-7.5 (Blight et al., 2002) was challenged with infectious HCVcc (Pietschmann et al., 2006), and the expression of cytokines and chemokines was measured (Figure S2A). At 48–72 hr after infection, transcripts of *LTα* (p = 0.05), *LTβ* (p = 0.05), *LIGHT* (p = 0.05), LTβR (p = 0.05), and chemokines (*CCL2*, *CCL3*, *CXCL1*, and *CXCL10*) were increased (2- to 32-fold) in HCVcc-infected, compared with noninfected Huh-7.5 cells.

Identification of Liver Cells Expressing LTβR and Its Ligands in HBV or HCV Infections

To identify the cellular source of *LTα*, *LTβ*, *LTβR*, and *LIGHT* expression in human HCV-infected livers, cells were collected from HCV-induced hepatitis and HCC (Figure 2A; Figure S2B). Liver cells were sorted according to their CD45 surface expression, resulting in CD45-enriched (T and B cells; monocytes, macrophages, and Kupffer cells; and dendritic and NK cells) or CD45-depleted (hepatocytes, oval cells, and bile duct epithelial and endothelial cells) fractions. Purity of these fractions was assessed by real-time PCR for lymphocyte (CD3, CD20, and CD45) or hepatocyte (cytokeratin 18) markers. CD45-depleted fractions displayed only a minor contamination with CD45 mRNA (~1%–10%), and CD45-enriched fractions showed only a minor amount of cytokeratin 18 mRNA transcripts (~2%–20%; Figure S2C; data not shown). Unsorted liver cells of healthy individuals were included as controls. Because of ethical

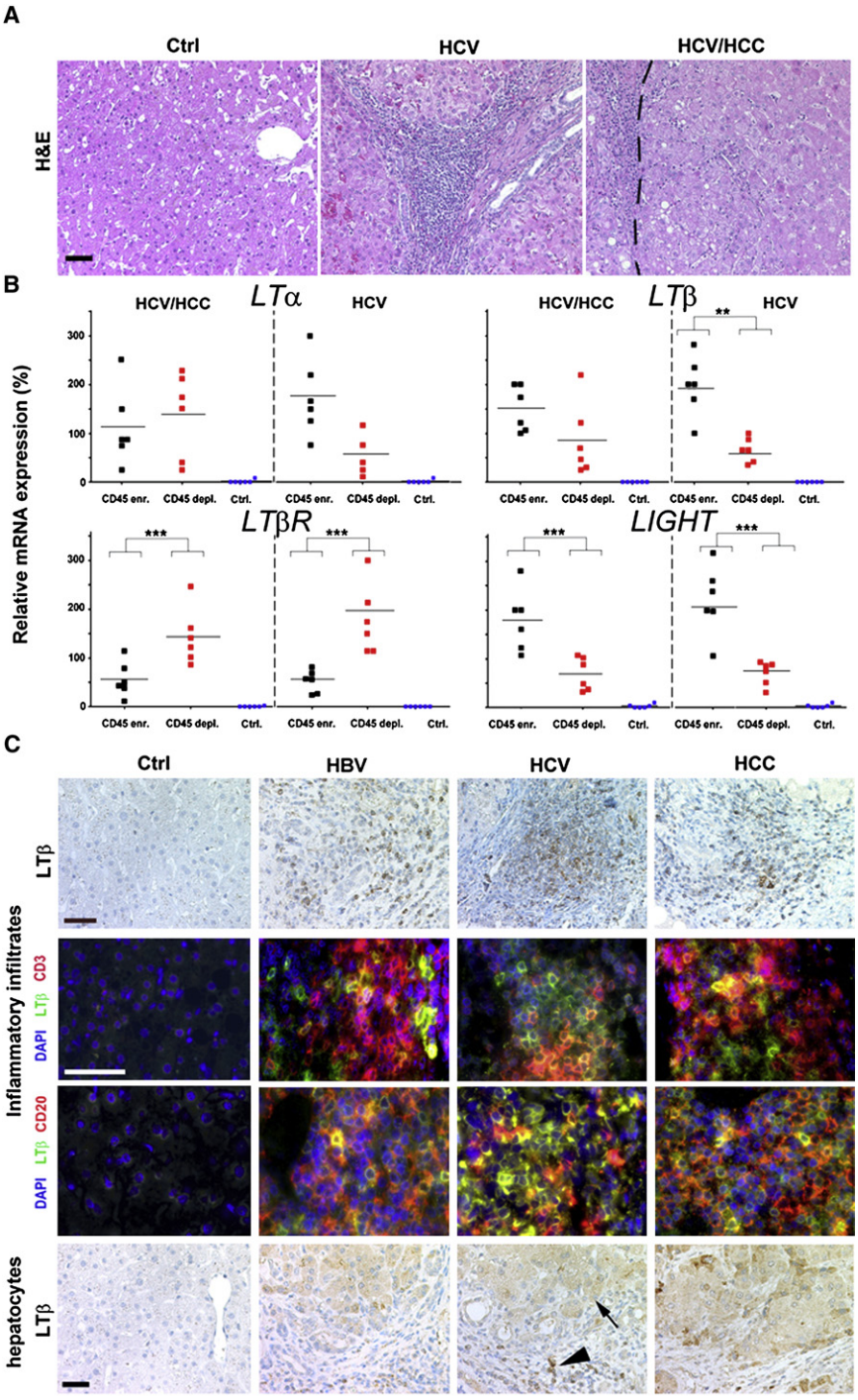

Figure 2. Identification of Cell Types Expressing Some TNF-Superfamily and TNF-Receptor-Superfamily Members in Virus-Infected or HCC-Affected Livers

(A) Histology of representative paraffin sections of healthy controls, HCV-infected livers, and HCC with HCV etiology. HCV-infected livers (HCV) and tumors (HCV/HCC) display leukocytic infiltrates. H&E, hematoxylin and eosin staining. The tumor border is indicated by a dashed line (scale bar, 100 μm).

(B) Real-time PCR analysis of sorted, CD45-enriched, or CD45-depleted liver cells. For control, whole liver cell populations derived from healthy or diseased livers (HCV infected/HCC) were used. mRNA expression levels are normalized to unsorted, total cell populations of the respective liver disease and calculated as 100%. The average expression level is indicated as percentage of control (unsorted cells of the respective disease) and demarcated by horizontal bars. Asterisks indicate statistical significance (Student's t test): *$p \leq 0.05$; **$p < 0.001$; ***$p < 0.0001$.

(C) Immunohistochemical (upper and lower panels) and immunofluorescence analysis for LTβ expression in healthy, HBV- or HCV-infected and HCC-affected livers (scale bar, 50 μm). Arrowhead depicts $LT\beta^+$ leukocytes, and an arrow depicts $LT\beta^+$ hepatocytes.

consideration, not enough human healthy liver tissue was available in order to perform cell sorting.

Within HCV-induced HCC, CD45-enriched and -depleted liver cells expressed similar *LTα* or *LTβ* mRNA levels (LTα, p = 0.8; LTβ, p = 0.1) that were significantly higher than in controls ($p < 0.0001$) (Figure 2A). *LTβR* mRNA transcript levels were significantly higher in CD45-depleted cells, compared with CD45-enriched cells (p = 0.006) or controls ($p < 0.0001$). In contrast, *LIGHT* mRNA expression was significantly increased in CD45-enriched cells when compared to CD45-depleted cells (p = 0.008) or controls (p = 0.0007).

Within HCV-induced hepatitis, CD45-enriched cells exhibited a trend toward increased *LTα* mRNA levels (p = 0.089) and a significant increase in both *LTβ* and *LIGHT* transcripts, compared with CD45-depleted cells (*LTβ*, p = 0.006; *LIGHT*, p = 0.01), or controls. Similar to HCV-induced HCC, *LTβR* mRNA expression was significantly higher in CD45-depleted cells than in CD45-enriched cells (p = 0.002) or controls ($p < 0.0001$). Thus, both CD45-enriched and CD45-depleted cell fractions express *LTα*, *LTβ*, and *LIGHT* in HCV-induced hepatitis and HCC.

Immunohistochemical analysis for LTβ protein expression corroborated these data: $CD3^+$ and $CD20^+$ lymphocytes and hepatocytes in HBV- or HCV-induced hepatitis and HCC, but not those in healthy liver specimens, express LTβ protein (Figure 2C).

Hepatocyte-Specific LTα and -β Overexpression Induces Chronic Progressive Hepatitis

To determine whether sustained hepatic LTβR signaling is causally linked to chronic hepatitis and liver cancer, we analyzed two

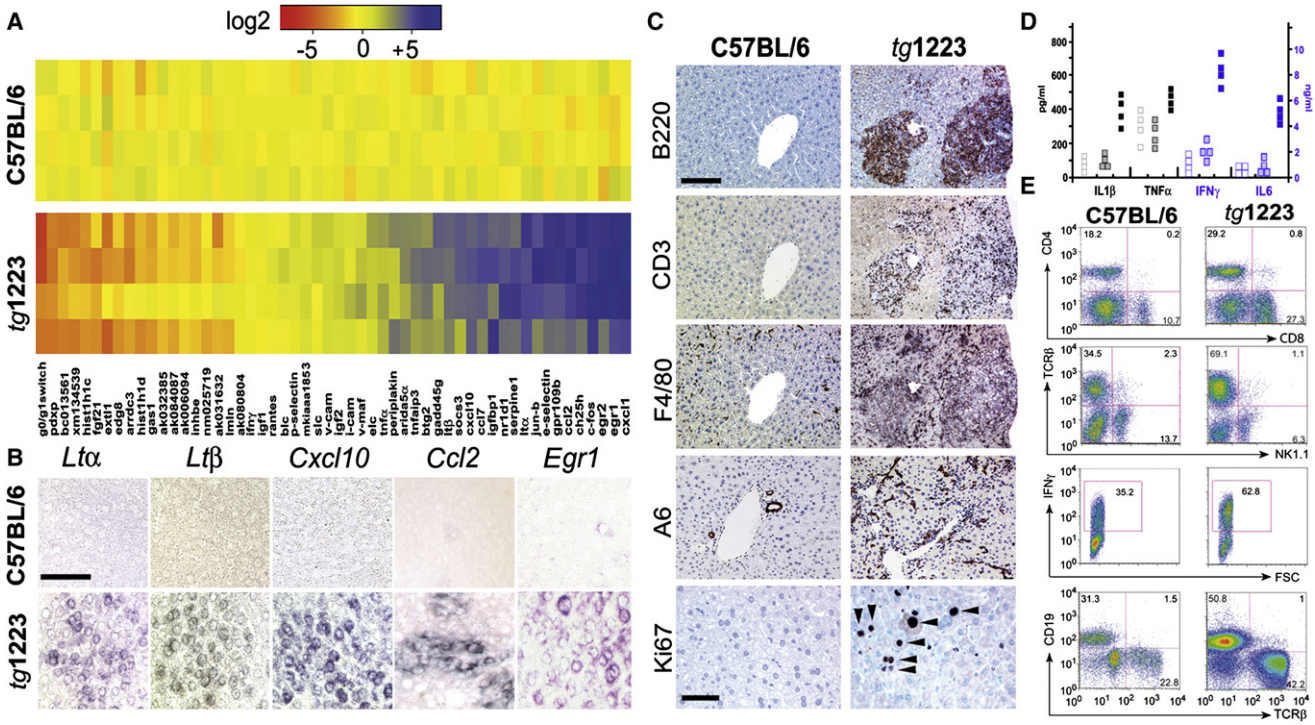

Figure 3. Characterization of Livers from *tg*1223 Mice

(A) Real-time PCR analysis for mRNA expression in liver of candidate genes at the age of 3 months. Data are presented in a $\log_2$ scale (blue, upregulated; red, downregulated). Rows indicate individual mice; columns represent particular genes. Each data point reflects the median expression of a particular gene resulting from three to four technical replicates, normalized to the mean expression value of the respective gene in C57BL/6 livers.

(B) In situ hybridization of C57BL/6 and *tg*1223 liver sections with *Ltα*, *Ltβ*, *Cxcl10*, *Ccl2*, and *Egr1* antisense probes (age of 3 months). Multiple scattered foci of hepatocyte-specific *Ltα*, *Ltβ*, *Cxcl10*, *Ccl2*, and *Egr1* mRNA were detected (scale bar, 50 μm).

(C) Immunohistochemical analysis of representative 9-month-old C57BL/6 and *tg*1223 livers. $B220^+$-stained B cells, $CD3^+$ T cells, $F4/80^+$ macrophages, Kupffer cells, and $A6^+$ oval cells (scale bar, 150 μm). $Ki67^+$ proliferating hepatocytes (arrow heads) and inflammatory cells are indicated (scale bar, 50 μm).

(D) ELISA for IL1β, TNFα, IFNγ, and IL6 in C57BL/6 (hollow symbols), *tg*1223 (filled symbols), or *tg*1222 (dotted symbols) liver homogenates (9 months).

(E) Flow cytometry of intrahepatic lymphocytes at 9 months of age: CD4 (T helper cells), CD8 (cytotoxic T cells), TCRβ (T cells), CD19 (B cells), IFNγ (Interferon γ). IFNγ expression was monitored on $CD4^+/CD8^+$ gated T cells. Representative flow cytometry analyses are shown. Numbers in each quadrant indicate the relative percentage of cells. Staining intensity is depicted on a log scale. FSC, forward scatter.

transgenic mouse lines that expressed LTα and -β in a liver-specific manner at low (*tg*1222) or high (*tg*1223) level (Heikenwalder et al., 2005). Although livers of *tg*1222 and *tg*1223 mice were histologically indistinguishable from those of control littermates at three months of age (Figure S3), the hepatic transcriptome was already considerably altered in *tg*1223 and to a lesser degree in *tg*1222 mice (Figure 3A; data not shown). Genes with the most dramatic expression changes were identified by DNA-microarray analysis and confirmed by real-time PCR (Figure 3A). As expected, *Ltα* and *Ltβ* transcripts were increased in *tg*1222 and *tg*1223 livers (Figure 3A; data not shown). Additionally, mRNA expression of chemokines (*Ccl2*, *Ccl7*, *Cxcl1*, and *Cxcl10*), genes involved in early growth response (e.g., *Egr1* and *Egr2*), cholesterol metabolism (e.g., *Ch25h*), and immediate early response (e.g., *c-Fos*, *Jun-b*, and *Socs-3*) were significantly ($p < 0.0001$) elevated. In contrast, genes involved in cell cycle control, histone modifications, and cell metabolism were significantly downregulated ($p < 0.0001$) (Figure 3A; Tables S6–S8 and Figure S4). In situ hybridization revealed *Ltα*, *Ltβ*, *Cxcl10*, *Ccl2*, and *Egr1* mRNA transcripts in hepatocytes of 3-month-old *tg*1223 mice (Figure 3B; Figure S3).

At the age of 4 months, a slight increase in intrahepatic $CD11b^+$, $CD68^+$, and $MHCII^+$ cells was detected in *tg*1223 mice, compared with age-matched *tg*1222 or C57BL/6 mice (Figure S3; data not shown). At this time point, no significant increase in IL1β, IFNγ, IL6, and TNFα protein levels was found (data not shown). At 4–6 months, transgenic livers started to develop strong portal and lobular (*tg*1223) or weak portal (*tg*1222) inflammation consisting of $CD4^+$, $CD8^+$ T cells, $B220^+$ B cells, and $CD11c^+$ dendritic cells (Figure S3; Heikenwalder et al., 2005).

At ≥9 months of age, *tg*1223 livers exhibited strong portal and lobular lymphocytic infiltrates (Figure 3C). A pronounced influx of $F4/80^+$ macrophages and proliferation of $A6^+$ oval cells was observed. Chronic inflammation coincided with increased proliferating $Ki67^+$ hepatocytes (*tg*1223, 17 ± 5 $Ki67^+$cells/mm^2 liver section; C57BL/6, 0.5 ± 0.3 $Ki67^+$cells/mm^2 liver section; $p = 0.003$), which was not significant in age-matched *tg*1222 livers ($p = 0.08$; Figure 3C; data not shown).

At this stage, hepatitis was accompanied by increased protein levels of IL1β ($p = 0.05$), IFNγ ($p = 0.05$), and IL6 ($p = 0.05$), and, to a lesser degree, TNFα in *tg*1223 livers. In *tg*1222 livers, we observed only a slight elevation of these cytokines, compared

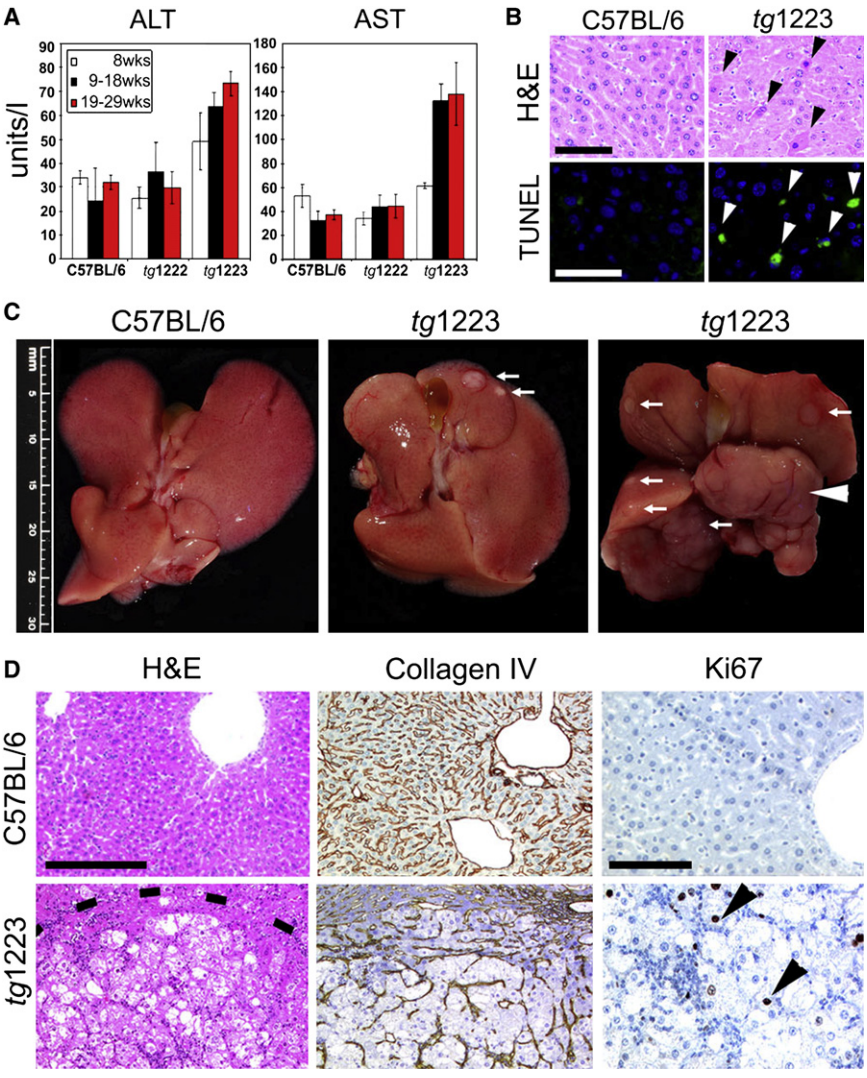

Figure 4. Chronic Liver Injury and HCC Development in *tg*1223 Mice

(A) Analysis of transaminase levels (ALT and AST) in sera of transgenic and control mice. Standard deviation (± SD) is indicated by error bars.

(B) Increased hepatocyte cell death in *tg*1223 livers documented by H&E staining and TUNEL/DAPI assay. Black arrowheads indicate apoptotic hepatocytes. TUNEL, green TUNEL$^+$ hepatocyte nuclei indicate apoptosis (white arrowheads; scale bars, 50 μm).

(C) Macroscopy of C57BL/6 (left panel) and *tg*1223 livers at the age of 12 (middle panel) and 18 months (right panel). White arrows indicate tumor nodules. White arrowhead indicates a liver lobe completely affected by HCC. Scale bar size is indicated.

(D) Histological analysis of livers derived from C57BL/6 and *tg*1223 mice. Dashed line depicts the HCC border. Collagen IV staining highlights the broadening of the liver cell cords and loss of collagen IV networks indicative of HCC in *tg*1223 mice (scale bar, 200 μm). High numbers of Ki67$^+$ proliferating hepatocytes (arrowheads) are only found in *tg*1223 HCC (right column; scale bar, 100 μm).

with C57BL/6 (Figure 3D). Quantitative analysis of total intrahepatic lymphocytes revealed an increase in *tg*1223 livers (C57BL/6, 17–24 × 10^6 cells/liver; *tg*1223, 35–73 × 10^6 cells/liver; $p < 0.05$). Intrahepatic lymphocytes were further characterized by flow cytometry (Figure 3E). Frequencies of CD8$^+$ (C57BL/6, 18% ± 11%; *tg*1223, 38% ± 10%), CD4$^+$ (C57BL/6, 16% ± 3%; *tg*1223, 26% ± 6%) and TCRβ$^+$ T cells (C57BL/6, 33.5% ± 9%; *tg*1223, 63.5% ± 4%) were elevated (n = 4), whereas NK1.1$^+$ cells (C57BL/6, 12% ± 2%; *tg*1223, 7% ± 2%) were reduced in *tg*1223 livers. Furthermore, an increase in the frequency of CD19$^+$ B cells was found in *tg*1223 livers (C57BL/6, 25% ± 7%; *tg*1223, 52% ± 4%). Elevated frequencies of IFNγ-producing CD4$^+$ and CD8$^+$ T cells were found in *tg*1223 mice, whereas IL17-producing cells remained unchanged (Figure 3E; data not shown).

LTα and LTβ Overexpression Induces Hepatotoxicity

To determine whether chronic hepatitis leads to hepatocyte cell death in *tg*1222 or *tg*1223 mice, we analyzed serum transaminase levels (ALT and AST). From the age of 19 weeks on, serum ALT and AST levels were significantly elevated ($p = 0.05$) in *tg*1223, but not in *tg*1222 mice (Figure 4A), and apoptotic hepatocytes were frequently detected in *tg*1223 mice (*tg*1223, 40.3 ± 11.4 TUNEL$^+$cells/mm^2 liver section; C57BL/6, 3.9 ± 6.2 TUNEL$^+$cells/mm^2 liver section; $p = 0.0005$), but rarely in *tg*1222 and virtually absent in C57BL/6 mouse livers from the age of 6 months on (Figure 4B; Figure S5; data not shown for *tg*1222).

Hepatitis persisted in both transgenic lines for ≥18 months. Phenotypes were much milder in *tg*1222 mice, implying that the LT expression level determined the severity of inflammation and liver injury. Therefore, *tg*1223 mice were selected for additional experiments, and further key results were obtained from this mouse line.

Microarray and real-time PCR analyses revealed elevated mRNA expression of genes involved in embryogenesis (e.g., *Dmrta1*), liver inflammation (e.g., *Pbfe1*), carcinogenesis (e.g., *Phlda3* and *Thrsp*; Kawase et al., 2009), glucose homeostasis and insulin sensitivity (e.g., *Fgf21*), and reduced mRNA expression of genes responsible for cell-cycle control (*Gadd45 g*) and protease inhibition (*SerpinA9*) in 9-month-old *tg*1223 livers, compared with C57BL/6 livers (Figure S5 and Tables S9–S11). Several genes were strongly up- or downregulated in 3-month-old *tg*1223 livers (Figure 3A) and returned to normal levels at 9 months, except that *Ltα* and -β mRNAs remained at high levels. On the other hand, genes involved in cell division, liver inflammation, lipid metabolism, wound healing, and tumorigenesis were significantly upregulated ($p < 0.001$), whereas genes involved in growth arrest and apoptosis were significantly downregulated ($p < 0.001$) in 9-month-old compared with 3-month-old *tg*1223 livers (Figure S5; Tables S12–S17).

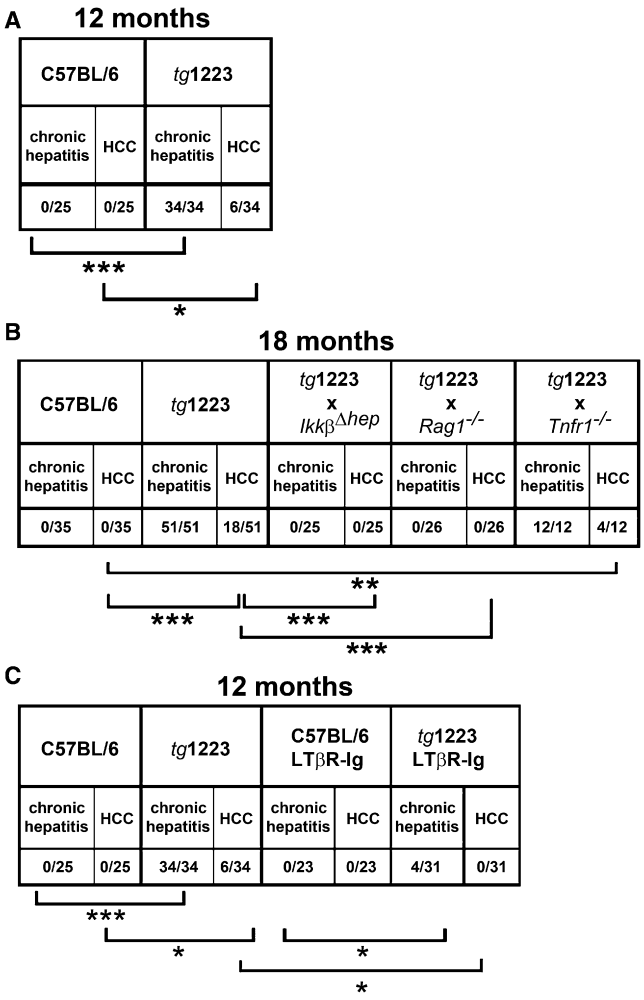

Figure 5. Chronic Hepatitis and HCC Incidence in *tg*1223 Mice, *tg*1223 Mice Intercrossed with Various Knockout Mice, and LTβR-Ig-Treated *tg*1223 Mice

(A) Chronic hepatitis and HCC incidence in 12-month-old *tg*1223 and C57BL/6 mice.

(B) Chronic hepatitis and HCC incidence in 18-month-old *tg*1223 and intercrossed *tg*1223 mice.

(C) Reduced chronic hepatitis and HCC incidence in 12-month-old *tg*1223 mice treated with LTβR-Ig. Statistical evaluation: asterisks indicate the degree of statistical significance. *$p < 0.05$; **$p < 0.001$; ***$p < 0.0001$.

HCC Development in *tg*1223 Mice

At 12 months of age, about 20% (6/34) of *tg*1223 mice developed macroscopically visible nodules that classified histologically as HCC, including broadening of liver cell cords, loss of collagen IV networks, and increased proliferative activity. In contrast, age-matched C57BL/6 livers lacked HCC (0/20; $p = 0.05$) (Figures 4C, 4D, and 5). Tumor frequency increased with age, reaching ~35% (18/51) by 18 months, whereas C57BL/6 mice did not develop HCC (0/35; $p < 0.0001$) (Figure 5; Figure S6). Tumors varied in size (1–25 mm), and histology and affected both sexes with similar frequencies (males:females = 13:11; $p = 0.3$) (Figure 4; Tables S18 and S19).

$A6^+$ oval cells (Engelhardt et al., 1990) were focally (8/24) or diffusely (2/24) distributed within some *tg*1223 HCC. The remaining *tg*1223 HCC (14/24) lacked $A6^+$ cells but were surrounded by them at the border zone of HCC (Figure S6).

Chromosomal Aberrations and Local Spread of HCC in *tg*1223 Mice

We further investigated microdissected *tg*1223 HCC (n = 9) and age-matched C57BL/6 livers (n = 5) for chromosomal aberrations. Array comparative genomic hybridization analysis (aCGH) revealed chromosomal aberrations in all *tg*1223 HCC (Figure 6). Amplifications and deletions of chromosomal regions ranged from ≤1 megabase (MB) to 160 MB and were detected in most autosomes of all analyzed *tg*1223 HCC. Of note, the pattern of chromosomal aberrations varied in HCC from different individual *tg*1223 mice ($p = 0.34$). aCGH analysis of independent C57BL/6 liver DNA samples did not reveal significant chromosomal aberrations.

We did not detect lung metastases but often saw multifocal intrahepatic disease in 18-month-old *tg*1223 mice. We therefore investigated whether multifocal *tg*1223 HCC represented intrahepatic spread of clonal tumors. Independent HCC (n = 6) from different lobes of the same *tg*1223 liver were microdissected and subsequently analyzed by aCGH. All HCC taken from the same liver displayed significantly overlapping chromosomal aberrations throughout the entire genome ($p < 0.05$), suggesting a clonal relationship of a tumor that has locally spread within the liver (Figure 6B).

Expression of Tumor Markers GP73, GS, and AFP in *tg*1223 HCC

We then evaluated expression of human liver tumor markers golgi protein 73 (GP73), glutamine synthetase (GS), and α-fetoprotein (AFP) in *tg*1223 livers (Bachert et al., 2007; Marrero and Lok, 2004; Sakamoto, 2009). GP73, GS, and AFP protein expression was elevated in most *tg*1223 HCC, as detected by immunohistochemistry and immunoblot analysis, compared with C57BL/6 livers or unaffected liver regions adjacent to HCC (Figures 7A–7C; data not shown).

Mechanisms Driving LTαβ-Induced Chronic Hepatitis and Liver Cancer

To identify other receptors and molecular mediators potentially involved in LT-induced chronic hepatitis and HCC development, we intercrossed *tg*1223 with *Tnfr1*$^{-/-}$, *Tnfr2*$^{-/-}$, or *Ikkβ*$^{\Delta hep}$ mice. The requirement of lymphocytes in chronic hepatitis and HCC formation was investigated by intercrossing with *Rag1*$^{-/-}$ mice, which lack mature lymphocytes.

The absence of IKKβ, TNFR1, or lymphocytes per se did not appear to influence transgenic *Lt*α and -β mRNA expression (Figures 3A and 7D). Initially, at 3 months of age, *tg*1223/*Ikkβ*$^{\Delta hep}$, *tg*1223/*Tnfr1*$^{-/-}$, *tg*1223/*Tnfr2*$^{-/-}$, and *tg*1223/*Rag1*$^{-/-}$ mice lacked histological evidence of hepatitis similar to *tg*1223 mice (data not shown). The aberrant hepatic gene expression pattern described for 3-month-old *tg*1223 mice developed only partially in *tg*1223/*Ikkβ*$^{\Delta hep}$ and *tg*1223/*Rag1*$^{-/-}$ mice, whereas *tg*1223/*Tnfr1*$^{-/-}$ livers displayed an expression profile similar to that of *tg*1223 mice (Figure 7D; Figure S7). At 9 months of age, *tg*1223/*Rag1*$^{-/-}$ (n = 26) and *tg*1223/*Ikkβ*$^{\Delta hep}$ (n = 18) livers lacked hepatitis, hepatocyte, or oval-cell proliferation (Figure S4), whereas *tg*1223/*Tnfr1*$^{-/-}$ (n = 8) or *tg*1223/*Tnfr2*$^{-/-}$ (n = 8) livers

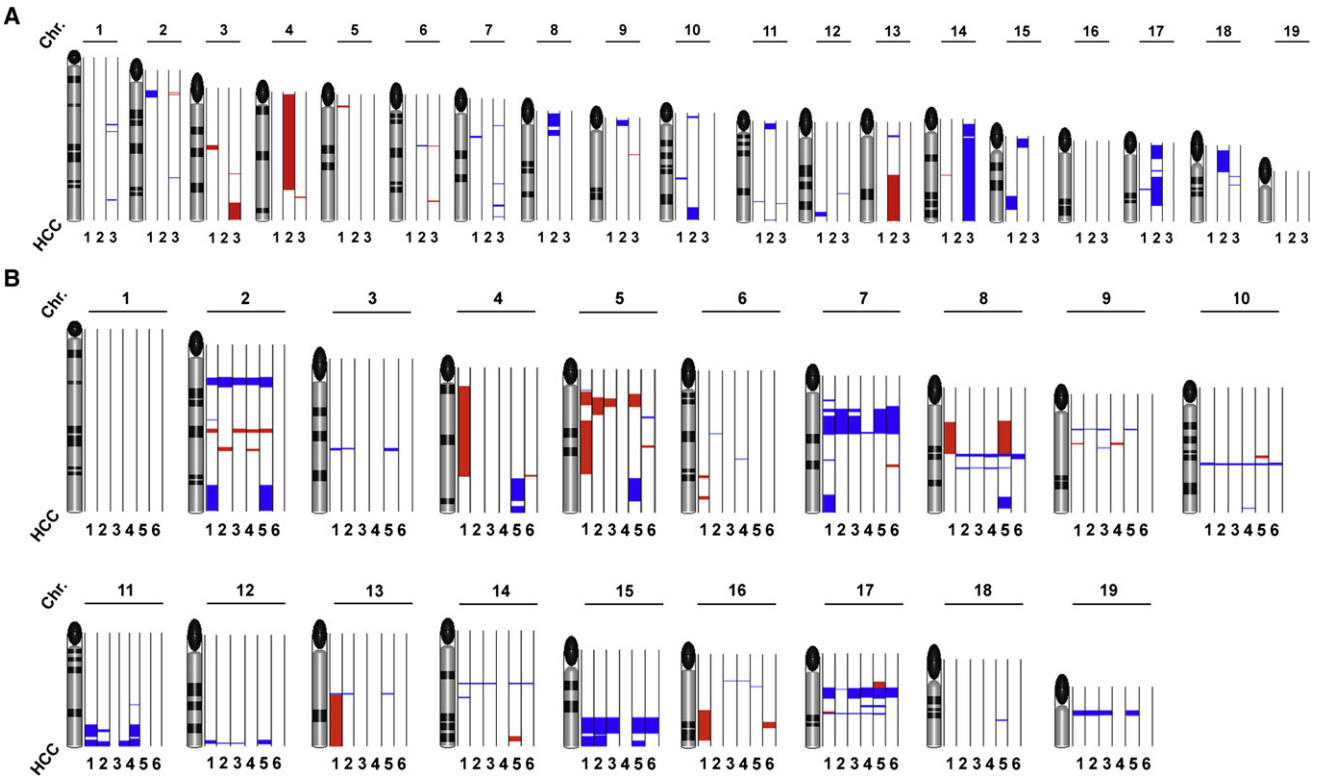

Figure 6. aCGH Analysis of HCC from *tg*1223 Mice

The q-arm of each chromosome is shown, and chromosome numbers are indicated. Black ellipses on the top of each q-arm represent the centromere. Dark horizontal bars within the symbolized chromosomes represent G bands. Chromosomal deletions are indicated in blue, and amplifications are indicated in red (see Experimental Procedures for details).

(A) HCC of individual *tg*1223 mice were hybridized against liver tissue of age-matched C57BL/6 mice and analyzed by aCGH analysis. Columns next to each chromosome represent individual HCC (1, 2, 3), with numerous chromosomal aberrations on the q-arm of various autosomes. No common pattern of chromosomal aberrations could be detected.

(B) aCGH analysis of six representative HCC (1, 2, 3, 4, 5, and 6) taken from different lobes of the same *tg*1223 liver.

were indistinguishable from those of *tg*1223 mice (Figure 3C and Figures 7E and 7F; Figure S7).

At the age of 18 months, *tg*1223/*Rag1*$^{-/-}$ (n = 26) and *tg*1223/*Ikkβ*$^{\Delta hep}$ (n = 25) mice were devoid of hepatitis and HCC ($p < 0.0001$) (Figures 5 and 7G), suggesting that both lymphocytes and hepatocyte-specific IKKβ expression are required for LT-induced chronic hepatitis and HCC development. Notably, *tg*1223/*Tnfr1*$^{-/-}$ mice displayed HCC (4/12) with an incidence similar to that among *tg*1223 mice (Figures 5 and 7G; Figure S8; Tables S18 and S19), indicating that TNFR1 signaling is not essential for LT-induced HCC formation in *tg*1223 mice.

Hepatocytes Are the Major Responsive Liver Cells to Agonistic LTβR Antibody Treatment

To investigate whether hepatocytes represent the major LT-responsive liver cells and to investigate LTβR signaling in *Tnfr1*$^{-/-}$ and *Ikkβ*$^{\Delta hep}$ livers, TNFα (positive control), agonistic LTβR antibody (3C8), and appropriate negative controls (PBS; rat IgG) were administered intravenously to C57BL/6 and various knockout mice (Figure 8; Figure S8). Nuclear p65 (RelA) translocation in hepatocytes and nonparenchymal cells (NPC, e.g., Kupffer cells and lymphocytes), alterations in the hepatic transcriptome, and protein expression of selected chemokines were examined.

Administration of 3C8 induced nuclear p65 translocation, primarily in hepatocytes and some NPC of C57BL/6 livers (Figure 8A), as well as transcriptional changes and upregulation of selected chemokines reminiscent of those observed in 3-month-old *tg*1223 livers (Figure 8A; Figure S9). Similar results were obtained after 3C8 treatment of *Tnfr1*$^{-/-}$ mice, in contrast to *Ikkβ*$^{\Delta hep}$ livers, which were devoid of nuclear p65 translocation in hepatocytes and NPC (Tables S20 and S21). Furthermore, upregulation of selected NF-κB target genes could not be detected. Control *Ltβr*$^{-/-}$ mice treated with 3C8 lacked nuclear p65 translocation in hepatocytes or NPC, as well as upregulation of selected NF-κB target genes.

To examine whether lack of functional IKKα on hepatocytes and NPC would suppress LTβR-induced upregulation of selected NF-κB responsive genes, we investigated livers of mice expressing a nonphosphorylatable *IKKα*^{AA} knockin allele (*Ikkα*$^{AA/AA}$; Cao et al., 2001). Upon 3C8 treatment, *Ikkα* $^{AA/AA}$ mice upregulated selected NF-κB responsive genes (Figure S8). The degree of mRNA upregulation in liver was similar to that in 3C8-treated C57BL/6 mice. In contrast, control treated (rat IgG) *Ikkα* $^{AA/AA}$

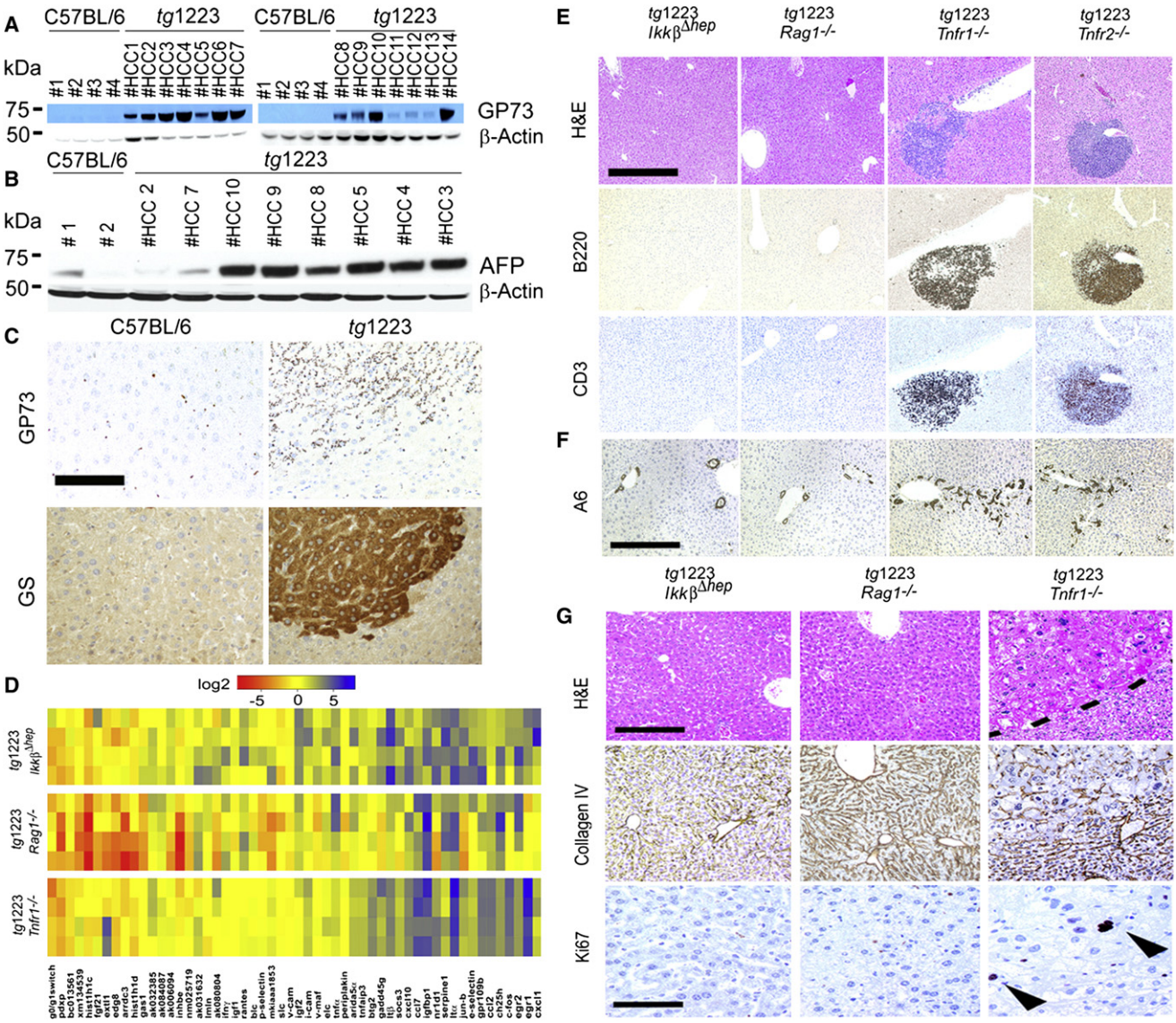

Figure 7. Expression of Tumor Markers in *tg*1223 HCC and Mechanistic Characterization of Liver Carcinogenesis in *tg*1223 Mice

(A) Immunoblot analysis of C57BL/6 and *tg*1223 HCC homogenates for GP73. Strong to moderate signal intensities were detected in all *tg*1223 HCC, but not in C57BL/6 livers.

(B) Immunoblot analysis of C57BL/6 and *tg*1223 HCC homogenates for AFP. β-Actin served as a loading control (kDa, kilo Dalton).

(C) Immunohistochemistry for GP73 and GS in a representative *tg*1223 HCC and age-matched C57BL/6 control (scale bar, 100 μm).

(D) mRNA expression of candidate genes in livers of 3-month-old *tg*1223/*Ikkβ*$^{\Delta hep}$, *tg*1223/*Rag1*$^{-/-}$, and *tg*1223/*Tnfr1*$^{-/-}$ mice. Data are presented in a $\log_2$ scale (blue, upregulated; red, downregulated). Rows indicate individual mice; columns represent particular genes. Each data point reflects the median expression of a particular gene resulting from three to four technical replicates, normalized to the mean expression value of the respective gene in C57BL/6 livers.

(E) Histological analysis of *tg*1223/*Ikkβ*$^{\Delta hep}$, *tg*1223/*Rag1*$^{-/-}$, *tg*1223/*Tnfr1*$^{-/-}$, and *tg*1223/*Tnfr2*$^{-/-}$ livers at 9 months of age. H&E, B220 for B cells and CD3 for T cells (scale bar, 500 μm).

(F) Immunohistochemical analysis of A6^{+} cells (oval cells) in livers of *tg*1223/*Ikkβ*$^{\Delta hep}$, *tg*1223/*Rag1*$^{-/-}$, *tg*1223/*Tnfr1*$^{-/-}$, and *tg*1223/*Tnfr2*$^{-/-}$ mice at 9 months of age (scale bar, 500 μm).

(G) Immunohistochemical analysis of *tg*1223/*Ikkβ*$^{\Delta hep}$, *tg*1223/*Rag1*$^{-/-}$, and *tg*1223/*Tnfr1*$^{-/-}$ livers (18 months of age). Dashed line depicts the HCC border (upper row; scale bar, 200 μm). Collagen IV staining highlights the broadening of liver cell cords and loss of collagen IV networks in *tg*1223/*Tnfr1*$^{-/-}$ HCC. Ki67^{+}-proliferating hepatocytes are indicated by arrowheads (lower row; scale bar, 50 μm).

mice lacked upregulation of selected NF-κB responsive genes. This finding suggests that 3C8-mediated hepatic LTβR signaling is mainly integrated by hepatocytes involving canonical NF-κB pathway.

Inhibition of LTβR Signaling Reduces Chronic Hepatitis and Carcinogenesis

We further investigated the involvement of LTβR signaling in the transition of chronic hepatitis to HCC by long-term LTβR-Ig

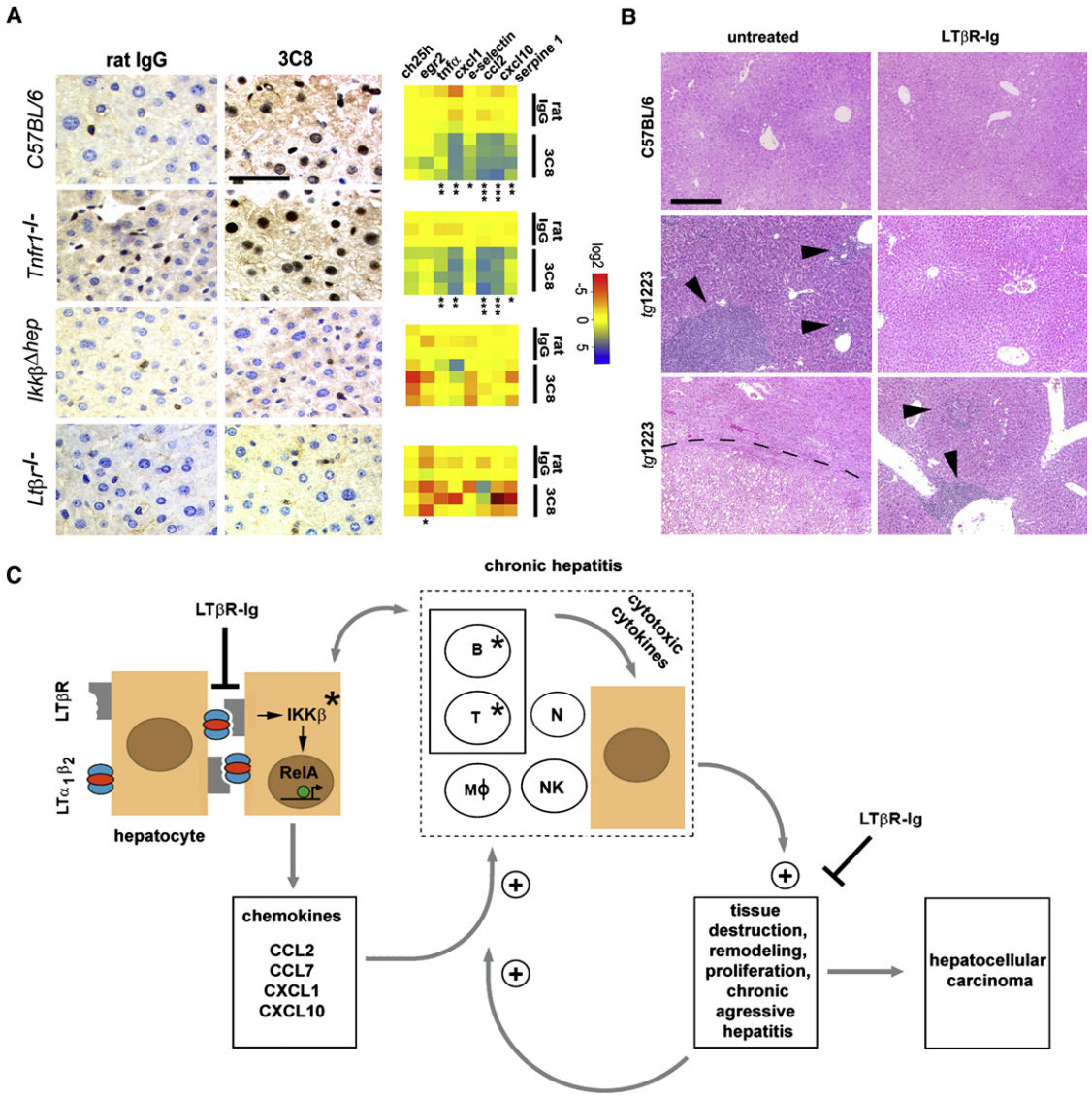

Figure 8. Effects of Acute 3C8 and Long-Term LTβR-Ig Treatment and a Model of Chronic Inflammation-Induced Hepatocarcinogenesis in *tg*1223 Mice

(A) Immunohistochemical analysis of nuclear p65 translocation and real-time PCR for mRNA expression of selected NF-κB target genes in livers of C57BL/6 and various knockout mice treated with 3C8. Data are presented on a $\log_2$ scale (blue, upregulated; red, downregulated). Rows indicate individual mice; columns represent particular genes. Each data point reflects the median expression value of a particular gene resulting from three to four technical replicates, normalized to the mean expression value of the respective gene in C57BL/6 livers. (scale bar, 50 μm). Expression data are depicted according to treatment group: rat IgG (control) or 3C8 (LTβR agonist). Statistical significance was evaluated by *t* test: $^{*}p \leq 0.05$; $^{**}p < 0.001$; $^{***}p < 0.0001$.

(B) Histological analysis (H&E) of livers from untreated (left column) and LTβR-Ig treated (right column) C57BL/6 or *tg*1223 mice (12 months of age). Representative sections show no hepatitis or HCC in untreated or LTβR-Ig-treated C57BL/6 livers (upper row). Untreated *tg*1223 livers display hepatitis in 34/34 (middle panel, left column) and HCC in 6/34 cases (lower panel, left column). LTβR-Ig treatment reduces the incidence of hepatitis (middle and lower panel, right column) and prevents HCC formation in LTβR-Ig treated *tg*1223 mice. Arrowheads indicate inflammatory foci. Tumor border is indicted by a dashed line (scale bar, 200 μm).

(C) Scheme of chronic inflammation-induced liver carcinogenesis in *tg*1223 mice: Transgenic hepatocytes (brown) express LTα and -β and induce chemokine production (e.g., CCL2, CCL7, CXCL1, and CXCL10) in the presence of IKKβ and intrahepatic lymphocytes. Chemoattraction and activation of myeloid cells and lymphocytes expressing particular chemokine receptors (e.g., CXCR3, CXCR2, CCR2, and CCR1) cause hepatitis: CXCL10 attracts $CXCR3^{+}$ T and NK cells, CXCL1 $CXCR2^{+}$ T cells, B cells, neutrophils, and CCL2 $CCR2^{+}$ macrophages, and CCL7 attracts $CCR1^{+}$ monocytes. Activated, infiltrating immune cells secrete cytotoxic cytokines (e.g., IL6, IL1β, TNFα, IFNγ, and LTαβ) that cause tissue destruction, hepatocyte proliferation, cell death, and tissue remodeling. In such an environment, hepatocytes are susceptible to chromosomal aberrations leading to HCC. Tissue destruction and remodeling supports the infiltration of activated inflammatory cells (e.g., myeloid cells), leading to a feed-forward loop toward chronic aggressive hepatitis. Asterisks indicate that genetic depletion of those components (IKKβ; T and B cells) blocks chronic hepatitis development and HCC. Blocking LTβR signaling with LTβR-Ig in 9-month-old *tg*1223 mice reduces chronic hepatitis incidence and prevents HCC. (+) indicates the fortification of a described process. (⊣) indicates the suppression of a described process. The transcription factor RelA is schematically depicted as a green circle, inducing transcription of NF-κB target genes (e.g., chemokines) (arrow). B, B cells; T, T cells; MØ, macrophages; N, neutrophils; NK, NK cells.

administration in *tg*1223 mice. Nine-month-old *tg*1223 mice with chronic hepatitis (n = 31) or age-matched C57BL/6 mice (n = 23) were treated with LTβR-Ig for 2 months, remained untreated for another 4 weeks, and then were sacrificed.

LTβR-Ig treatment significantly reduced chronic hepatitis incidence in *tg*1223 mice, compared with that in untreated *tg*1223 mice (treated, 4/31; untreated, 34/34; $p < 0.0001$). Furthermore, LTβR-Ig treatment suppressed chronic hepatitis-driven HCC formation (treated, 0/31; untreated, 6/34; $p < 0.05$) (Figures 5 and 8B). LTβR-Ig treatment did not lead to overt histopathological alterations in C57BL/6 livers or overt changes in lymphocyte (B and T cells) or macrophage populations within spleens of C57BL/6 or *tg*1223 mice (data not shown). Efficiency of LTβR-Ig treatment was ascertained by the loss of LTβR-dependent follicular dendritic cells (FDCs) within C57BL/6 and *tg*1223 spleens (Figure S9). Thus, our results imply that long-term suppression of LTβR reduces chronic hepatitis incidence and can prevent the transition from chronic hepatitis to HCC in *tg*1223 mice.

DISCUSSION

This study uncovered drastic and robust mRNA upregulation of *LTβR*, *LTα*, and *LTβ* in HBV- or HCV-induced hepatitis and HCC. *LT* and *LIGHT* transcripts were mainly expressed by $CD3^+$ T cells and $CD20^+$ B cells; a significant proportion of *LTα* and *LTβ* expression was also attributable to hepatocytes. Notably, upregulation of *LTβR*, *LTα*, and *LTβ* transcripts was also detected in non-virus-related HCC, which could stem from activated, tumor-infiltrating lymphocytes and/or from neoplastic hepatocytes that have upregulated LT, possibly in response to IL6. It was demonstrated that HCC-derived cell lines express IL6 (Baffet et al., 1991) and that LT levels are increased in response to IL6 in the latter (Subrata et al., 2005).

LT signaling induces both canonical and noncanonical NF-κB signaling pathways, whose role in controlling liver cancer formation remains controversial (Vainer et al., 2008). In a mouse model with acute DEN exposure, depletion of functional NF-κB signaling ($Ikk\beta^{\Delta hep}$ mice) increased hepatocyte cell death, enhanced Kupffer cell activation, and elevated HCC incidence (Maeda et al., 2005). In contrast, NF-κB signaling promotes HCC development in $mdr2^{-/-}$ mice (Pikarsky et al., 2004), and hepatocyte-specific depletion of IKKβ prevents HCC formation in *tg*1223 mice. How can this contradictory role of IKKβ signaling in HCC formation be reconciled? On the one hand, IKKβ signaling might be required for hepatocytes to appropriately respond to and survive carcinogenic stimuli and acute liver injury (e.g., DEN exposure). On the other hand, IKKβ signaling might enable chemokine expression by hepatocytes, leading to hepatitis and HCC. Consistent with this hypothesis, *tg*1223/$Rag1^{-/-}$ mice were devoid of chronic hepatitis, hepatocyte, or oval-cell proliferation and failed to develop HCC.

Why could immune cells contribute to liver tumorigenesis? One explanation might be that $CD4^+$ or $CD8^+$ T cells expressing inflammatory cytokines (e.g., IL1β, TNFα, and IFNγ), as well as cytolytic proteins (e.g., Granzyme B), contribute to hepatocyte cell death, tissue remodeling, and transformation, finally leading to HCC (Budhu and Wang, 2006; Nakamoto et al., 1998). Intrahepatic lymphocytes may also influence the production of inflammatory mediators, because 3-month-old *tg*1223/$Rag1^{-/-}$ livers displayed markedly reduced cytokine and chemokine levels.

We propose that, rather than directly acting as a cell-autonomous oncogene on hepatocytes or $A6^+$ oval cells, hepatic LTαβ expression induces local upregulation of chemokines (e.g., *Ccl2*, *Cxcl10*, *Cxcl1*, and *Ccl7*) by hepatocytes. This leads to the attraction of circulating inflammatory cells and a hyperproliferative, hepatotoxic environment stochastically leading to HCC formation (Figure 8C). It is worth mentioning that some chemokines found in this study (e.g., CXCL10) have been reported to be mainly expressed by human hepatocytes in chronic hepatitis C (Zeremski et al., 2007).

Ablation of TNFR1 signaling did not prevent chronic hepatitis and HCC formation in *tg*1223 mice, although anti-TNFα antibody treatment prevents HCC development in $mdr2^{-/-}$ mice (Pikarsky et al., 2004). We investigated the mode of LT signaling in $Tnfr1^{-/-}$ livers upon 3C8 treatment. This treatment induced analogous hepatic changes seen in *tg*1223 mice at 3 months of age. Similar to our results with *tg*1223/$Tnfr1^{-/-}$ mice, this finding suggests that heterotrimeric LT causes p65 translocation in hepatocytes and induces a TNFR1-independent signaling cascade via LTβR, presumably contributing to chronic hepatitis and HCC. Most probably, HCC formation in $mdr2^{-/-}$ mice depends on pathways involving TNFR1 distinct from the LTβR-dependent pathways described in our study.

Intravenous administration of TNFα into $Ikk\beta^{\Delta hep}$ mice did not cause p65 translocation in hepatocytes but upregulated NF-κB target genes, presumably through TNFα-activated NPC. In contrast, 3C8 treatment in $Ikk\beta^{\Delta hep}$ mice had no effect. Therefore, hepatocytes but not NPC are likely to be the major liver cells integrating LT signaling. Interestingly, upon 3C8 treatment, $Ikk\alpha^{AA/AA}$ livers upregulated selected NF-κB target genes, similar to C57BL/6 mice (Figure S8). Therefore, the absence of *IKKα* in hepatocytes and NPC allows NF-κB target gene expression upon 3C8 treatment, suggesting the involvement of the classical NF-κB pathway in LTβR-induced hepatic signaling.

LTβR signaling was reported to induce oval-cell proliferation (Akhurst et al., 2005), which is thought to contribute to the development of liver tumors (Lee et al., 2006). We observed proliferation of $A6^+$ oval cells in chronically inflamed *tg*1223 livers at the age of 9 months and found $A6^+$ cells within and at the border of *tg*1223 HCC. Whether those $A6^+$ cells represent transformed oval cells contributing to liver carcinogenesis or whether A6 is upregulated on aberrant hepatocytes within HCC remains to be determined.

Lack of lymphocytes or chronic hepatitis prevented oval-cell proliferation, although LTα and β transgene expression was unaltered. Therefore, it is conceivable that activated, infiltrating lymphocytes or Kupffer cells may contribute to oval cell proliferation by providing further LT or other cytokines in *tg*1223 livers. On the basis of the presented data, a sequence of events leading to chronic hepatitis and HCC in *tg*1223 mice can be proposed (Figure 8C).

What are the possible clinical implications of our findings? It has recently been demonstrated that pharmacological inhibition of LTβR signaling reduces virus-, bacteria-, and concavalin A–induced liver injury (An et al., 2006; Anand et al., 2006; Puglielli et al., 1999), whereas triggering LTβR signaling on hepatocytes appears to be beneficial during liver regeneration (Tumanov

et al., 2008). Moreover, siRNA knock-down of various components of the LTβR signaling pathway (e.g., LTβ and RelA) were shown to interfere with HCV replication in vitro (Ng et al., 2007). Therefore, inhibition of LTβR signaling might also impede the efficiency of HCV replication.

What are the possible side effects of blocking LTβR signaling? The reported effects include alterations in the microarchitecture of white pulp follicles and disappearance of FDC networks in nonhuman primates (Gommerman et al., 2002). Of note, despite the loss of FDCs and a reduced capacity to trap immune complexes, the primary antibody response to keyhole limpet hemocyanin was not significantly altered (Gommerman et al., 2002).

Accordingly, we have investigated a possible beneficial effect of blocking LTβR signaling in *tg*1223 mice with chronic hepatitis. This partially reverted inflammation and prevented HCC formation, suggesting that LTβR-Ig treatment might be beneficial in liver pathologies with sustained LT signaling.

Our results show that LT signaling is critically involved in hepatitis and subsequent HCC development and imply that blocking LTβR signaling might become a beneficial therapeutic approach in the context of HBV- or HCV-induced chronic hepatitis and other liver diseases displaying sustained hepatic LTβR signaling.

EXPERIMENTAL PROCEDURES

Human Liver Tissue

Human liver biopsy specimens were obtained from University Hospitals Zurich, Freiburg, Grenoble, Heidelberg, and Graz. Biopsy specimens were registered in the respective biobanks and kept anonymous. The research project was authorized by the ethical committees of the "Gesundheitsdirektion Kanton Zürich" (Ref. Nr. StV 26-2005), Freiburg (Nr. 299/2001), Heidelberg (Prof. Bannasch), Graz (Ref. Nr. 1.0 24/11/2008), and Grenoble (Ref. Nr. 03/APTF/1). The study protocol was in accordance with the ethical guidelines of the Helsinki declaration. Patients were enrolled after giving their written informed consent. HBV- or HCV-infected patients with chronic hepatitis were not treated with ribavirin or other immunomodulatory drugs at the time point of needle biopsy.

Mice

Animals were maintained under specific pathogen–free conditions, and experiments were approved and conform with the guidelines of the Swiss Animal Protection Law, Veterinary office, Canton Zurich. Mouse experiments were performed under licenses 198/2007, 83/2007, and 30/2005 according to the regulations of the Veterinary office of the Canton Zurich. *Tg*1223, *tg*1222, *Tnfr1*$^{-/-}$, *Tnfr2*$^{-/-}$, *Rag1*$^{-/-}$, *Ltβr*$^{-/-}$, *Ikkα*$^{AA/AA}$, and *Ikkβ*$^{\Delta hep}$ mice were generated as previously published (Bluethmann et al., 1994; Cao et al., 2001; Futterer et al., 1998; Heikenwalder et al., 2005; Maeda et al., 2005; Mombaerts et al., 1992).

TNFα and 3C8 Treatment

Twelve-to-fourteen-week-old male mice (C57BL/6 and knock-out mice) were intravenously injected with either PBS, murine recombinant TNFα (50 μg/kg bodyweight; R&D Systems), agonistic LTβR antibody (50 μg/mouse; clone 3C8; eBioscience), or rat IgG (50 μg/mouse; eBioscience) and sacrificed for analysis 45 min after injection. All substances were injected at a total volume of 100 μl dissolved in PBS.

Isolation of Intrahepatic Murine Lymphocytes

Mice were anesthetized, and liver was perfused with PBS to remove circulating leukocytes; then isolated liver tissue was minced and digested in medium containing collagenase (1 mg/ml) and DNase (25 μg/ml) at 37°C for 40 min. Cells were centrifuged at 300 rpm for 3 min to sediment the majority of hepatocytes. Supernatant was removed and centrifuged again at 1200 rpm for 10 min. Cell pellet was resuspended in the 40% fraction of a 40:80 Percoll gradient. Upon centrifugation at 2500 rpm for 20 min, intrahepatic murine lymphocytes (IHLs) were collected at the interface. IHLs were analyzed for surface marker expression by staining with anti-CD4, anti-CD8, anti-TCR-β, anti-NK1.1, or anti-CD19 antibodies (Abs), and for cytokine production capacity by intracellular staining with anti-IFNγ and anti-IL17 Abs (all from eBioscience) upon PMA/Ionomycin stimulation for 4 hr by using a two-laser FACScalibur (BD). Analysis was executed with CellQuest and FlowJo software.

Measurement of Aminotransferases

The analysis for AST and ALT was performed with mouse serum on a Roche Modular System (Roche Diagnostics) with a commercially available automated colorimetric system at the Institute of Clinical Chemistry at the University Hospital Zurich using a Hitachi P-Modul (Roche).

ACCESSION NUMBERS

Gene expression microarray data are deposited in the ArrayExpress database under accession number E-MEXP-1998. aCGH data are deposited in the GEO database under accession number GSE 14467.

SUPPLEMENTAL DATA

Supplemental data include Supplemental Experimental Procedures, nine figures, and 21 tables and may be found with this article online at http://www.cell.com/cancer-cell/supplemental/S1535-6108(09)00294-3.

ACKNOWLEDGMENTS

We thank Birgit Riepl, Mareike Schroff, Manja Barthel, Petra Schwarz, Marianne König, Rita Moos, Udo Ungethüm, Mirzet Delic, Urs Egli, Silvia Behnke, André Fitsche, Andrea Patrignani, Marie-Ange Thelu, and Gitta Selezznik for excellent technical assistance. We thank the members of the LT team at Biogen Idec for LT reagents; Annette Schmitt-Graeff for performing Knodell score analysis; and Wolfram Jochum, Tracy O'Connor, Stefan Zoller, Thomas Fuchs, Holger Moch, Glen Kristiansen, Peter Schraml, Thomas Ried, Claude Carnaud, Helmut Denk, Christopher Soll, Evelyne Jouvin-Marche, and Burkhardt Seifert for discussions. We thank Peter Bannasch for providing human tissues, Valentina Factor for antibodies (A6), and Alexei Tumanov (mLtα, mLtβ), Wolf-Dietrich Hardt (mCxcl10), Barrett Rollins (mCcl2), and Volkhard Lindner (mEgr1) for providing plasmids. We thank Jean-Pierre Zarski, Vincent Leroy, and Christian Letoublon from Michallon Hospital in Grenoble. This study was supported by grants of the Oncosuisse foundation OCS 02113-08-2007 (M.H., A.W., and M.O.K.), the Bonizzi-Theler foundation (M.H.), the "Stiftung zur Schweizerischen Krebsbekämpfung" (M.H.), the research foundation at the Medical Faculty Zurich (J.B. and M.H.), the "Kurt und Senta Hermann Stiftung" (M.H. and J.H.), the Austrian Genome Programme GEN-AU (K.Z.), the Swiss National Science Foundation (A.A.), the Agence Nationale pour la Recherche sur le Sida (ANRS), and from Pole de Compétitivité LyonBiopole (P.N.M.). M.J.W. was supported by a grant of the Roche Research Foundation. SN is HHMI International Research Scholar. M.R. was supported by the Higher Education Commission of Pakistan. M.H. is a fellow of the Prof. Dr. Max Cloëtta foundation.

Received: January 6, 2009
Revised: June 20, 2009
Accepted: August 24, 2009
Published: October 5, 2009

REFERENCES

Akhurst, B., Matthews, V., Husk, K., Smyth, M.J., Abraham, L.J., and Yeoh, G.C. (2005). Differential lymphotoxin-beta and interferon gamma signaling during mouse liver regeneration induced by chronic and acute injury. Hepatology *41*, 327–335.

An, M.M., Fan, K.X., Cao, Y.B., Shen, H., Zhang, J.D., Lu, L., Gao, P.H., and Jiang, Y.Y. (2006). Lymphtoxin beta receptor-Ig protects from T-cell-mediated liver injury in mice through blocking LIGHT/HVEM signaling. Biol. Pharm. Bull. *29*, 2025–2030.

Anand, S., Wang, P., Yoshimura, K., Choi, I.H., Hilliard, A., Chen, Y.H., Wang, C.R., Schulick, R., Flies, A.S., Flies, D.B., et al. (2006). Essential role of TNF family molecule LIGHT as a cytokine in the pathogenesis of hepatitis. J. Clin. Invest. *116*, 1045–1051.

Bachert, C., Fimmel, C., and Linstedt, A.D. (2007). Endosomal trafficking and proprotein convertase cleavage of cis Golgi protein GP73 produces marker for hepatocellular carcinoma. Traffic *8*, 1415–1423.

Baffet, G., Braciak, T.A., Fletcher, R.G., Gauldie, J., Fey, G.H., and Northemann, W. (1991). Autocrine activity of interleukin 6 secreted by hepatocarcinoma cell lines. Mol. Biol. Med. *8*, 141–156.

Blight, K.J., McKeating, J.A., and Rice, C.M. (2002). Highly permissive cell lines for subgenomic and genomic hepatitis C virus RNA replication. J. Virol. *76*, 13001–13014.

Bluethmann, H., Rothe, J., Schultze, N., Tkachuk, M., and Koebel, P. (1994). Establishment of the role of IL-6 and TNF receptor 1 using gene knockout mice. J. Leukoc. Biol. *56*, 565–570.

Browning, J.L., and French, L.E. (2002). Visualization of lymphotoxin-beta and lymphotoxin-beta receptor expression in mouse embryos. J. Immunol. *168*, 5079–5087.

Browning, J.L., Sizing, I.D., Lawton, P., Bourdon, P.R., Rennert, P.D., Majeau, G.R., Ambrose, C.M., Hession, C., Miatkowski, K., Griffiths, D.A., et al. (1997). Characterization of lymphotoxin-alpha beta complexes on the surface of mouse lymphocytes. J. Immunol. *159*, 3288–3298.

Budhu, A., and Wang, X.W. (2006). The role of cytokines in hepatocellular carcinoma. J. Leukoc. Biol. *80*, 1197–1213.

Cao, Y., Bonizzi, G., Seagroves, T.N., Greten, F.R., Johnson, R., Schmidt, E.V., and Karin, M. (2001). IKKalpha provides an essential link between RANK signaling and cyclin D1 expression during mammary gland development. Cell *107*, 763–775.

Chen, C.M., You, L.R., Hwang, L.H., and Lee, Y.H. (1997). Direct interaction of hepatitis C virus core protein with the cellular lymphotoxin-beta receptor modulates the signal pathway of the lymphotoxin-beta receptor. J. Virol. *71*, 9417–9426.

El-Serag, H.B., and Rudolph, K.L. (2007). Hepatocellular carcinoma: epidemiology and molecular carcinogenesis. Gastroenterology *132*, 2557–2576.

Engelhardt, N.V., Factor, V.M., Yasova, A.K., Poltoranina, V.S., Baranov, V.N., and Lasareva, M.N. (1990). Common antigens of mouse oval and biliary epithelial cells. Expression on newly formed hepatocytes. Differentiation *45*, 29–37.

Fu, Y.X., Huang, G., Wang, Y., and Chaplin, D.D. (1998). B lymphocytes induce the formation of follicular dendritic cell clusters in a lymphotoxin alpha-dependent fashion. J. Exp. Med. *187*, 1009–1018.

Futterer, A., Mink, K., Luz, A., Kosco-Vilbois, M.H., and Pfeffer, K. (1998). The lymphotoxin beta receptor controls organogenesis and affinity maturation in peripheral lymphoid tissues. Immunity *9*, 59–70.

Gommerman, J.L., Mackay, F., Donskoy, E., Meier, W., Martin, P., and Browning, J.L. (2002). Manipulation of lymphoid microenvironments in nonhuman primates by an inhibitor of the lymphotoxin pathway. J. Clin. Invest. *110*, 1359–1369.

Greten, F.R., and Karin, M. (2004). The IKK/NF-kappaB activation pathway-a target for prevention and treatment of cancer. Cancer Lett. *206*, 193–199.

Heikenwalder, M., Zeller, N., Seeger, H., Prinz, M., Klohn, P.C., Schwarz, P., Ruddle, N.H., Weissmann, C., and Aguzzi, A. (2005). Chronic lymphocytic inflammation specifies the organ tropism of prions. Science *307*, 1107–1110.

Kawase, T., Ohki, R., Shibata, T., Tsutsumi, S., Kamimura, N., Inazawa, J., Ohta, T., Ichikawa, H., Aburatani, H., Tashiro, F., and Taya, Y. (2009). PH domain-only protein PHLDA3 is a p53-regulated repressor of Akt. Cell *136*, 535–550.

Lee, J.S., Heo, J., Libbrecht, L., Chu, I.S., Kaposi-Novak, P., Calvisi, D.F., Mikaelyan, A., Roberts, L.R., Demetris, A.J., Sun, Z., et al. (2006). A novel prognostic subtype of human hepatocellular carcinoma derived from hepatic progenitor cells. Nat. Med. *12*, 410–416.

Lee, S.H., Park, S.G., Lim, S.O., and Jung, G. (2005). The hepatitis B virus X protein up-regulates lymphotoxin alpha expression in hepatocytes. Biochim. Biophys. Acta *1741*, 75–84.

Lo, J.C., Wang, Y., Tumanov, A.V., Bamji, M., Yao, Z., Reardon, C.A., Getz, G.S., and Fu, Y.X. (2007). Lymphotoxin beta receptor-dependent control of lipid homeostasis. Science *316*, 285–288.

Lowes, K.N., Croager, E.J., Abraham, L.J., Olynyk, J.K., and Yeoh, G.C. (2003). Upregulation of lymphotoxin beta expression in liver progenitor (oval) cells in chronic hepatitis C. Gut *52*, 1327–1332.

Luedde, T., Beraza, N., Kotsikoris, V., van Loo, G., Nenci, A., De Vos, R., Roskams, T., Trautwein, C., and Pasparakis, M. (2007). Deletion of NEMO/IKK-gamma in liver parenchymal cells causes steatohepatitis and hepatocellular carcinoma. Cancer Cell *11*, 119–132.

Maeda, S., Kamata, H., Luo, J.L., Leffert, H., and Karin, M. (2005). IKKbeta couples hepatocyte death to cytokine-driven compensatory proliferation that promotes chemical hepatocarcinogenesis. Cell *121*, 977–990.

Malhi, H., Gores, G.J., and Lemasters, J.J. (2006). Apoptosis and necrosis in the liver: a tale of two deaths? Hepatology *43*, S31–S44.

Marrero, J.A., and Lok, A.S. (2004). Newer markers for hepatocellular carcinoma. Gastroenterology *127*, S113–S119.

Mombaerts, P., Iacomini, J., Johnson, R.S., Herrup, K., Tonegawa, S., and Papaioannou, V.E. (1992). RAG-1-deficient mice have no mature B and T lymphocytes. Cell *68*, 869–877.

Nakamoto, Y., Guidotti, L.G., Kuhlen, C.V., Fowler, P., and Chisari, F.V. (1998). Immune pathogenesis of hepatocellular carcinoma. J. Exp. Med. *188*, 341–350.

Ng, T.I., Mo, H., Pilot-Matias, T., He, Y., Koev, G., Krishnan, P., Mondal, R., Pithawalla, R., He, W., Dekhtyar, T., et al. (2007). Identification of host genes involved in hepatitis C virus replication by small interfering RNA technology. Hepatology *45*, 1413–1421.

Pietschmann, T., Kaul, A., Koutsoudakis, G., Shavinskaya, A., Kallis, S., Steinmann, E., Abid, K., Negro, F., Dreux, M., Cosset, F.L., and Bartenschlager, R. (2006). Construction and characterization of infectious intragenotypic and intergenotypic hepatitis C virus chimeras. Proc. Natl. Acad. Sci. USA *103*, 7408–7413.

Pikarsky, E., Porat, R.M., Stein, I., Abramovitch, R., Amit, S., Kasem, S., Gutkovich-Pyest, E., Urieli-Shoval, S., Galun, E., and Ben-Neriah, Y. (2004). NF-kappaB functions as a tumour promoter in inflammation-associated cancer. Nature *431*, 461–466.

Puglielli, M.T., Browning, J.L., Brewer, A.W., Schreiber, R.D., Shieh, W.J., Altman, J.D., Oldstone, M.B., Zaki, S.R., and Ahmed, R. (1999). Reversal of virus-induced systemic shock and respiratory failure by blockade of the lymphotoxin pathway. Nat. Med. *5*, 1370–1374.

Rennert, P.D., Browning, J.L., Mebius, R., Mackay, F., and Hochman, P.S. (1996). Surface lymphotoxin alpha/beta complex is required for the development of peripheral lymphoid organs. J. Exp. Med. *184*, 1999–2006.

Ruddell, R.G., Mann, D.A., and Ramm, G.A. (2008). The function of serotonin within the liver. J. Hepatol. *48*, 666–675.

Sakamoto, M. (2009). Early HCC: diagnosis and molecular markers. J. Gastroenterol. *44* (*Suppl 19*), 108–111.

Subrata, L.S., Lowes, K.N., Olynyk, J.K., Yeoh, G.C., Quail, E.A., and Abraham, L.J. (2005). Hepatic expression of the tumor necrosis factor family member lymphotoxin-beta is regulated by interleukin (IL)-6 and IL-1beta: transcriptional control mechanisms in oval cells and hepatoma cell lines. Liver Int. *25*, 633–646.

Tumanov, A.V., Koroleva, E.P., Christiansen, P.A., Khan, M.A., Ruddy, M.J., Burnette, B., Papa, S., Franzoso, G., Nedospasov, S., Fu, Y.X., and Anders, R.A. (2008). T cell-derived lymphotoxin regulates liver regeneration. Gastroenterology *136*, 694–704.

Tumanov, A.V., Kuprash, D.V., and Nedospasov, S.A. (2003). The role of lymphotoxin in development and maintenance of secondary lymphoid tissues. Cytokine Growth Factor Rev. *14*, 275–288.

Vainer, G.W., Pikarsky, E., and Ben-Neriah, Y. (2008). Contradictory functions of NF-kappaB in liver physiology and cancer. Cancer Lett. *267*, 182–188.

Ware, C.F. (2005). Network communications: lymphotoxins, LIGHT, and TNF. Annu. Rev. Immunol. *23*, 787–819.

You, L.R., Chen, C.M., and Lee, Y.H. (1999). Hepatitis C virus core protein enhances NF-kappaB signal pathway triggering by lymphotoxin-beta receptor ligand and tumor necrosis factor alpha. J. Virol. *73*, 1672–1681.

Zeremski, M., Petrovic, L.M., and Talal, A.H. (2007). The role of chemokines as inflammatory mediators in chronic hepatitis C virus infection. J. Viral Hepat. *14*, 675–687.

Zhu, N., Khoshnan, A., Schneider, R., Matsumoto, M., Dennert, G., Ware, C., and Lai, M.M. (1998). Hepatitis C virus core protein binds to the cytoplasmic domain of tumor necrosis factor (TNF) receptor 1 and enhances TNF-induced apoptosis. J. Virol. *72*, 3691–3697.